Final Draft
of the original manuscript:

Polymer architecture versus chemical structure as adjusting tools for the enzymatic degradation of oligo(ε-caprolactone) based films at the air-water interface

Anne-Christin Schöne[1,2], Karl Kratz[2], Burkhard Schulz[1,2], Andreas Lendlein[1,2*]

[1] Institute of Chemistry, University of Potsdam, Karl-Liebknecht-Str. 24-25, 14476 Potsdam, Germany

[2] Institute of Biomaterial Science and Berlin-Brandenburg Centre for Regenerative Therapies (BCRT), Helmholtz-Zentrum Geesthacht, Kantstr. 55, 14513 Teltow, Germany

*E-mail: andreas.lendlein@hzg.de

Abstract

The enzymatic degradation of oligo(ε-caprolactone) (OCL) based films at the air-water interface is investigated by Langmuir monolayer degradation (LMD) experiments to elucidate the influence of the molecular architecture and of the chemical structure on the chain scission process. For that purpose, the interactions of 2D monolayers of two star-shaped poly(ε-caprolactone) (PCLs) and three linear OCL based copolyesterurethanes (P(OCL-U)) with the lipase from *Pseudomonas cepacia* are evaluated in comparison to linear OCL. While the architecture of star-shaped PCL Langmuir layers slightly influences their degradability compared to OCL films, significantly retarded degradations are observed for P(OCL-U) films containing urethane junction units derived from 2, 2 (4), 4-trimethyl-hexamethylene-diisocyanate (TMDI), hexamethylene diisocyanate (HDI) or lysine ethyl ester diisocyanate (LDI). The enzymatic degradation of the OCL based 2D structures is related to the presence of hydrophilic groups within the macromolecules rather than to the packing density of the film or to the molecular weight. The results reveal that the LMD technique allows the parallel analysis of both the film/enzyme interactions and the degradation process on the molecular level.

1

1 Introduction

Poly(ε-caprolactone) (PCL) is a semi-crystalline polymer which is hydrolytically degradable [1]. It is explored for various biomedical applications especially when a slower degradation is required compared to glycolide based copolymers. The fine tuning of degradation rates and mechanical characteristics to the specific demands of each medical application is a continuous challenge in biomaterial science. Here, we consider variations both in the polymer architecture and the chemical structure of junction units to influence the degradation behavior. The molecular architecture is changed from linear to star-shaped.

Star-shaped macromolecules, which can be achieved by the use of polyvalent initiators[2], often exhibit unique physical properties[3,4] in solution, in bulk state[5] and at the air-water interface[6]. For example, star-shaped PCL exhibited decreased crystallization temperatures and a reduced degree of crystallinity with increasing the number of arms between one and five [7,8]. On the contrary, star-shaped PCL structures with 6 arms showed a slower crystallization than the less branched PCL[9], having similar crystalline structure revealed by X-ray diffractograms and polarized optical microscopy[7].

The synthesis of multiblock copolymers based on oligomeric OCL precursors is another established way to alter the molecular morphology and in this way to tune the mechanical properties, water absorption or degradation behavior [10-12]. Among them, the synthesis of copolyesterurethanes is explored to create highly elastic degradable biomaterials. In contrast to star-shaped PCL, polyesterurethanes prepared from PCL segments and diisocyantes show a decreasing crystallization tendency [13-15].

The hydrolytic degradation of PCL is slow compared to polyesters based on lactic and glycolic acid. But different types of lipases were able to catalytically accelerate the degradation process for instance, the lipase from *Humicola lanuginosa*, *Pseudomonas alcaligenes*, or *Pseudomonas cepacia* [16-20]. The lipases contain a catalytic triade consisting of serine, histidine and asparagine as the active site for hydrolyzing ester bonds [21-23].

2

Thin films often behave different than the bulk material, they exhibit unique surface structures and properties [24-26]. The Langmuir technique enables the preparation and investigation of 2D films from macromolecules, which can be studied as model systems for the formation of phase morphologies and degradation behavior [27]. The Langmuir monolayer degradation (LMD) technique was established as a suitable method to investigate the hydrolysis of polyesters at the air-water interface. The formation of water-soluble products in the degrading 2D film allows a fundamental understanding of the chain cleavage mechanism of polyester monolayers because the differentiation of the chain cleavage process from the diffusion of water and intermediate products as in 3D samples are no longer required [28-30]. For linear PCL in hydrolytic and enzymatic LMD experiments in combination with improved data acquisition the influence of subphase pH and temperature, enzyme concentration, and surface pressure of polymer chains on the degradation kinetics have been elucidated [30]. An exponential increase in the number of dissolved degradation fragments with increasing degradation time was determined and a random chain scission process was ascertained as the dominant scission mechanism.

Only a few studies on star-shaped polymers have been performed at the air-water interface in general. For PCL Langmuir layers it was shown that the degree of functionalization (one to three end groups) had a direct effect on the interfacial and superficial properties due to the modified hydrophobicity by the end groups [31]. The interfacial behavior of a PCL/poly(ethylene oxide) (PEO) based five-arm star-shaped block copolymer has been studied and compared to the film morphology of the corresponding LB films characterized by AFM. The copolymers undergo a phase transition, which corresponds to the degree of crystallization of the PCL blocks [32].

Enzymatic degradation experiments in bulk of various star-shaped PCL 3D films were performed using polymers with the same overall molecular weight (M_n = 10.300 g·mol^{-1}) but various arm numbers using the lipase from *Pseudomonas cepacia* [8]. While the degradation

rate increases with the number of arms from one to three, it decreases from three to five arms. This behavior is attributed to the crystal size or crystallinity and the limiting effect of the central core on chain mobility in star-shaped PCLs. From those bulk experiments it was not possible to differentiate between the molecular (architectural) and the morphological (crystallinity) factors on the degradation mechanism of star-shaped polymers. To get a deeper understanding of the different contribution of these parameters we investigated in this work Langmuir films based on oligo(ε-caprolactone) (OCL) at the air-water interface, which allow to avoid effects of crystallization processes on the enzymatic degradation. Therefore, the interfacial properties and the monolayer degradation behavior of star-shaped PCL with three- and four-arms compared with linear OCL-diols are elucidated. Oligo(ε-caprolactone) based copolyesterurethanes P(OCL-U)s are included to differentiate in degradation experiments between the influence of the molecular weight of the polymers and the film packing density. Thereby, only OCL sequences with comparable molecular weight in all molecules were used, which is schematically illustrated in Fig. 1. The influence of the urethane junction units on the packing motifs in a 2D OCL layer was shown previously [33] and it is assumed that the different packing motifs in the monolayers also influence the film degradation rate. By the LMD studies the impact of intra- and intermolecular interactions on the degradation behavior can be separated from crystallization effects as they occur in bulk.
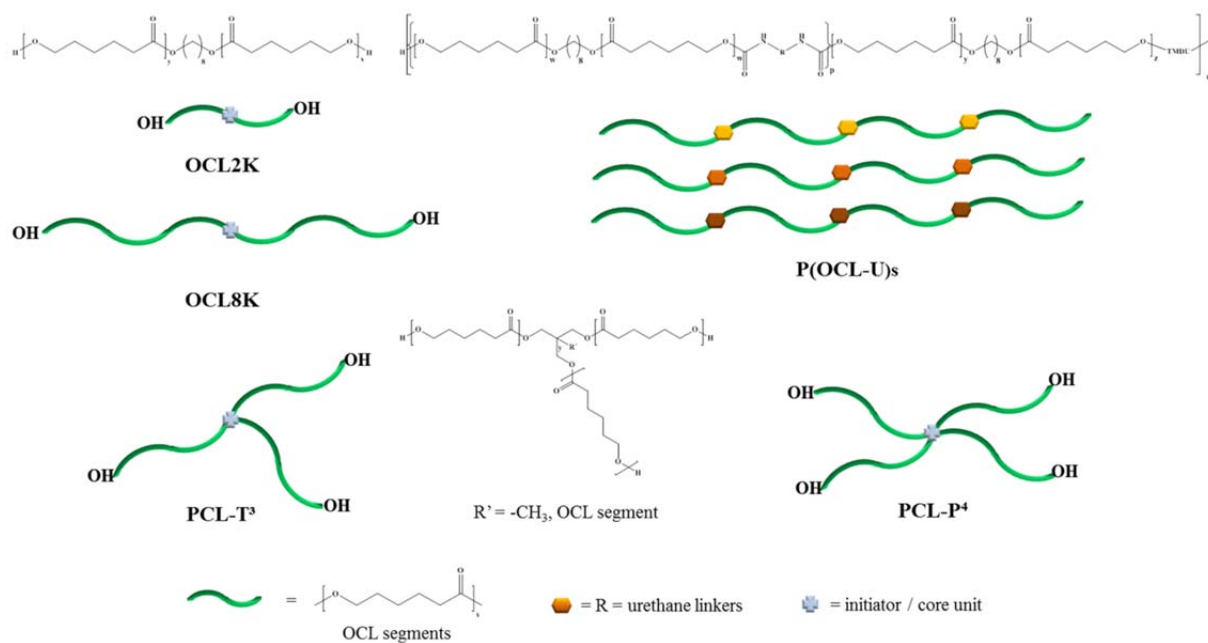
Fig. 1 Schematic illustration of OCL based molecules with different architectures, but similar OCL segments: diols, star-shaped, and polyesterurethanes containing different urethane junction units

2 Experimental part

2.1 Materials Oligo(ε-caprolactone)s (OCL) were purchased by Solvay Caprolactones, Warrington, U.K. (OCL2K: M_n = 2800 g·mol^{-1}, trade name CAPA2304, and OCL8K: M_n = 8300 g·mol^{-1}, trade name CAPA2803). Star-shaped polymers based on ε-caprolactone with three- and four-arms were synthesized using the catalyst dibutyltin oxide and the initiators trimethylolethane (three-arms: PCL-T³) and pentaerythritol (four-arms: PCL-P^4) [34]. The copolyesterurethanes were synthesized via co-condensation of the macrodiol oligo(ε-caprolactone) (M_n = 2000 g·mol^{-1}, trade name CAPA2205, Solvay Caprolactones, Warrington, U.K.) with of one of the diisocyanates hexamethylene diisocyanate (HDI), 2, 2 (4), 4-trimethyl hexamethylene diisocyanat (TMDI), or lysine ethyl ester diisocyanate (LDI) (all Sigma Aldrich) resulting in the multiblock copolymers P(OCL-HDU), P(OCL-TMDU), and P(OCL-LDU), respectively. From the ^{1}H-NMR spectra a high degree of functionalization of the initiator by ε-caprolactone chains (PCL-T³: 91%, PCL-P^4: 98%) was determined (see Supporting information Figs. S4 and S5). For the star-shaped and linear PCL the average number molecular weights (M_n), determined by gel permeation chromatography (GPC), ^{1}H-NMR, and OH-group titration, the polydispersity indices (PDI), and the numbers of end groups are summarized in Table 1. The urethane linked PCLs have an average number molecular weights of 40.000, 48.000 and 55.000 g·mol^{-1} for P(OCL-TMDU), P(OCL-HDU), and P(OCL-LDU), respectively, determined by GPC. GPC was performed with a multi detector set-up using chloroform at 35 °C as eluent with a flow rate of 1 mL·min^{-1} and 0.2 *wt*-% toluene as internal standard. Two detectors were used: a RI detector Shodex RI-101 (Showa Denko, Japan) and the viscosimeter SEC-3010 (WGE, Dr. Bures, Dallgow, Germany). The molecular weights were determined using a universal calibration with polystyrene standard.

Table 1 Number-average molecular weight (M_n) of linear OCLs and star-shaped PCLs with an error of 3% determined by GPC, ^{1}H-NMR and OH-value titration, the polydispersity index (PDI), number of end groups and average molecular weight per polymer arm.

Sample	M_n(GPC) [g·mol^{-1}]	PDI	OH-value [g·mol^{-1}]	M_n [g·mol^{-1}] [a]	No. of end groups	M_n(GPC) per end group [g·mol^{-1}]
OCL2K	2800	1.3	2700	2800	2	1400
OCL8K	8300	1.2	8000	8800	2	4000
PCL-T[3]	6600	1.2	8000	7800	3	2200
PCL-P[4]	13.000	1.4	21.700	19.300	4	3200

[a] Determined by ^{1}H-NMR using a Bruker Avance 300 spectrometer (300 MHz, in CDCl$_3$ (VWR, 99.8 %) at 25 °C, for more details see Supporting information).

The content of hydroxyl groups (OH-value) were determined as the hydroxyl number ($mg_{KOH}/g_{polymer}$) by potentiometric titration of the polymers dissolved in dimethylformamide (DMF, Merck), with 0.1 N tetrabutylammonium hydroxide (Merck). The titrations were performed with the titrator DMS Titrino 716 (Metrohm, Schwizerland) and a Solvotrode with LiCl (sat.) in ethanol at ambient temperature.

All polymers were used without any further purification. Chloroform (HPLC grade, Carl Roth, Germany) was used as spreading solvent. The aqueous subphase for the monolayer experiments was provided by a Milli-Q Gradient A-10 water purification system (Millipore, Merck, Germany).

2.2 Langmuir film balance The surface pressure-area (π-A) isotherms were recorded with a Langmuir trough ("Large" and "High compression" trough, KSV NIMA, Finland). The system was placed on an active vibration isolation system (halcyonics variobasic 40, Accurion, Germany) within a laser safety cabinet. The surface pressure (π) was measured by the Wilhelmy technique with a calibrated sensor located in the center between the barriers. The Langmuir trough was filled with de-ionized water (Millipore, Milli-Q *Gradient*, 18.2 MΩ·cm, toc < 4 ppb). The trough was cleaned thoroughly with chloroform (HPLC grade,

Roth). Afterwards, the trough was filled with deionized water. By monitoring the surface pressure the purity of the trough and the subphase was controlled. While closing the barriers, the total change of the surface pressure π should be below $\Delta\pi \leq 0.2$ mN·m^{-1}. For all OCL based samples the chloroform stock solutions had a concentration in the range of 0.45-0.75 mg·mL^{-1}. The solution was applied drop-wise onto the air-water interface using a microsyringe (Hamilton Co., Reno, NV, USA). Before an experiment was started the chloroform was allowed to evaporate for ten minutes. The polymer films were compressed and expanded with a constant compression rate of 10 mm·min^{-1}. The surface pressure was recorded as a function of the mean molecular area per repeating unit (MMA). All experiments were repeated at least three times. All presented isotherm data were reproducible with a random measurement error of 5% concerning the surface pressure or the MMA values for these independently repeated experiments.

All Langmuir monolayer degradation experiments are performed on a phosphate buffered system with the lipase *Pseudomonas cepacia* at 22 °C or 37 °C at a surface pressure of $\pi = 7$ mN·m^{-1}. Based on surface area reduction data, the corrected area reduction $\Delta A_{corr}(t)$ is calculated according to equation (1), where A(0) is the initial surface area occupied by the compressed monolayer (A(t = 0)) and A(t) is the required surface area after a certain degradation time interval t (Fig. 5b) [29]. $\Delta A_{corr}(t)$ allows the correlation between the surface area reduction data and the formation rate of water-soluble species per mean molecular area per repeating unit.

$$\Delta A_{corr}(t) = (A(0) \cdot A(t)^{-1}) - 1 \tag{1}$$

2.3 Brewster Angle Microscopy Studies (BAM) BAM images (500×400 μm²) were recorded with ellipsometer nanofilm_ep3 (EP3, Accurion, Göttingen, Germany) equipped with a high performance CCD camera (765 x 572 pixel), a 10x magnification lens with a maximum lateral resolution of 2 μm, and a 658 nm class IIIB laser source.

3 Results and Discussion

Surface pressure-area (π-A) isotherms are recorded for two star-shaped PCLs and compared to linear OCLs to get information about monolayer behavior of the star-shaped polymers at the air-water interface. The slopes of the isotherms on pure water at 22 °C are comparable to those of linear OCLs but, shifted to smaller MMA values with increasing arm number (Fig. 2). The inflection point (MMA_i at π_i) of the π-A isotherm representing the closest packing in the monolayer is determined from the maximum of the elasticity modulus κ ($\kappa = -A^{-1} (\delta\pi \, \delta A^{-1})$), which increases with increased number of arms (Fig. S6). We use the MMA_i values as measure for the film packing density because in all polymers investigated here the molecular weight of the OCL segments is comparable. As we have shown earlier, linear PCL exhibit a 2D-2D transition during compression characterized by converting from a "*side-on*" to an "*edge-on*" orientation based on the elliptical shape of the polymer chains [33]. For the closest packing in the Langmuir film a surface area between $MMA_{side-on} \sim 42 \text{ Å}^2$ and $MMA_{edge-on} \sim 34 \text{ Å}^2$ is derived from the crystal structure for an orthorhombic unit cell in bulk PCL [35, 36]. For both star-shaped PCLs the MMA_i are slightly smaller as in the "*edge-on*" orientation (Table 2). We assume that the core units and the OH-end groups in the star-shaped molecules contribute to the area reduction, while the OCL segments remain at the air-water interface in more stretched conformation. This behavior corresponds to bulk crystallization studies, where the core unit is pressed out of the lamellar crystals and a limited effect of the central core on the chain mobility results [8]. It is worth mentioning that 3D crystallization within the monolayer near the inflection point can be excluded in our experiments by BAM and does not contribute to the observed shift of the π-A isotherms.
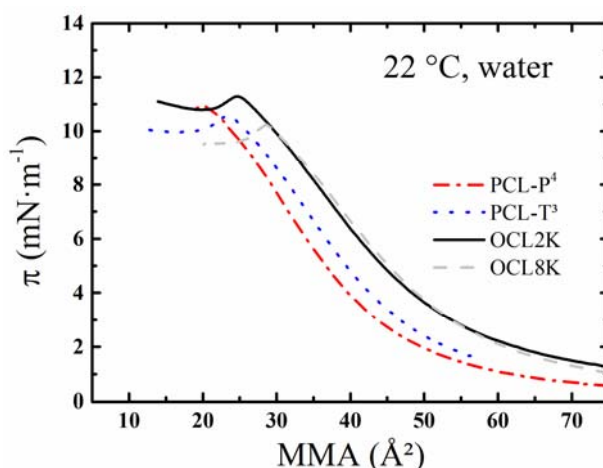
Fig. 2 π-A isotherms of OCL2K, OCL8K, PCL-T[3] and PCL-P[4] at 22 °C on a pure aqueous subphase (pH = 5.7).

Table 2 Langmuir monolayer characterization of star-shaped polymers based on PCL and linear OCLs by using the MMA_i value [Å^2] and the corresponding surface pressure π_i [mN·m^{-1}] determined at 22 °C on a water subphase and at 22 °C and 37 °C on a phosphate buffered saline (PBS) subphase.

Sample ID	MMA_i	π_i	MMA_i	π_i	MMA_i	π_i
	water, 22 °C		PBS, 22 °C		PBS, 37 °C	
OCL2K	39	6.6	39	6.6	36	6.4
OCL8K	37	7.1	38	7.0	37	6.4
PCL-T[3]	32	7.8	50	7.8	50	7.0
PCL-P[4]	30	7.5	52	7.2	52	6.8

With respect to the enzymatic degradation experiments, the π-A isotherms are also recorded on PSB buffered subphase at 22 °C and 37 °C (Fig. 3). The isotherm of two linear OCLs is inserted as a reference. Surprisingly, the π-A isotherms of the star-shaped PCLs at 22 °C are distinctly shifted to larger MMA_i values compared to linear OCL although the overall shape of the isotherm is unaffected (Table 2). Since this effect is only observed for the star-shaped PCL the increased number of hydrophilic end groups seems to be the crucial factor. We assume that the interactions of the polymer monolayer with the Na^{2+} and K^+ ions in the PBS buffer lead to the formation of partially charged end groups. As a consequence, a close interdigital packing of the arms is prevented by electrostatic repulsions between the molecules and results in a more spread 2D structure which is unable to be packed as dense as linear OCL molecules. This is confirmed by the fact that at 37 °C compared to 22 °C the positions of the

10

isotherms and the MMA_i values (Table 2) are unchanged, because ionic interaction are less sensitive to temperature effects. Interestingly, BAM images show crystalline structures in PCL-P[4] films above the inflection points comparable to linear OCLs. The crystallization behavior of the star-shaped PCL is not in the focus of the present investigation and therefore it will be described elsewhere.
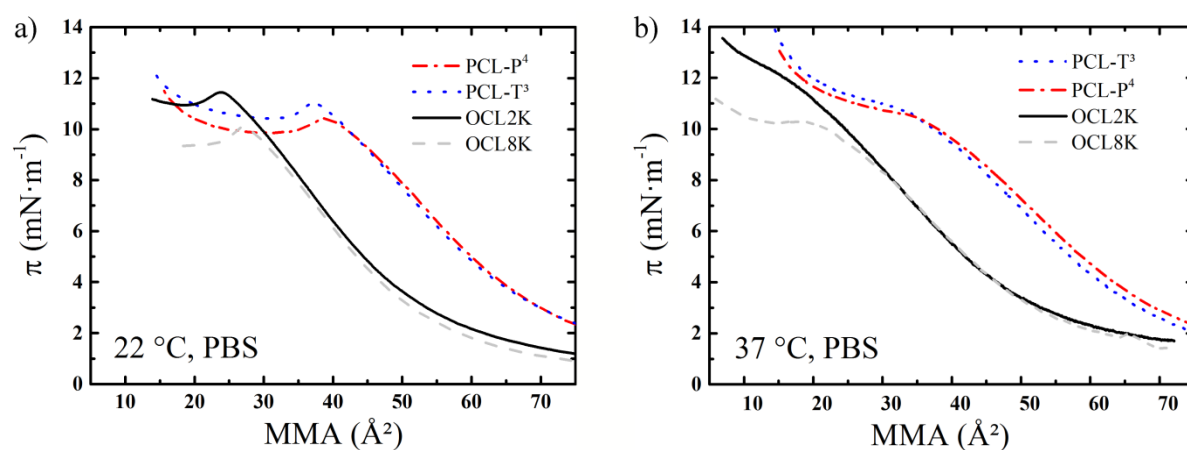

Fig. 3 π-A isotherms of PCL based material at 22 °C (a) and 37 °C (b) on a PBS buffered subphase for PCL-T[3] and PCL-P[4] compared with linear OCL2K and OCL8K.

Before enzymatic degradation experiments are performed, it was verified that no hydrolytic degradation occurs for star-shaped PCL based films in a time range of 4 h.

The surface area reduction data for the enzymatic degradation of the star-shaped PCLs are recorded at 37 °C on a PBS buffered system. After injection of the enzyme into the buffered subphase a fast decrease of the surface area is observed in approximately 20 min (Fig. S7). The used lipase from *Pseudomonas cepacia* has a high ability to degrade linear PCL by random chain scission mechanism suggesting an enhanced degradation rate of films with lower film packing densities caused by more statistical breaks per molecule. Surprisingly, the observed formation of water-soluble degradation fragments for the two star-shaped PCL is significantly slower compared to linear OCLs (Fig. 4a). The reason for this effect cannot be a difference in the molecular weights per OCL segment as the data in Table 1 show. The two

investigated linear OCLs have different molecular weights per end group, which cover the molecular weight range per arm for both star-shaped PCLs (OCL2K has a smaller and OCL8K has a larger average number molecular weight per end group). Considering this fact, the LMD experiments clearly point out that the shape influences the enzymatic degradation rate of PCL at the air-water interface at 37 °C rather than the molecular weight. The reason might be the packing motifs in the 2D monofilm at the air-water interface. At 22 °C the overall degradation rate for PCL-T³ is still in the same range compared to OCL whereas for PCL-P[4] a decreased degradation velocity is observed independent of the packing density as visible in the π-A isotherm. That means that the degradation behavior (Fig. 4b) is influenced by the molecular architecture of PCL in a similar manner as known from bulk investigation at 37 °C [8].
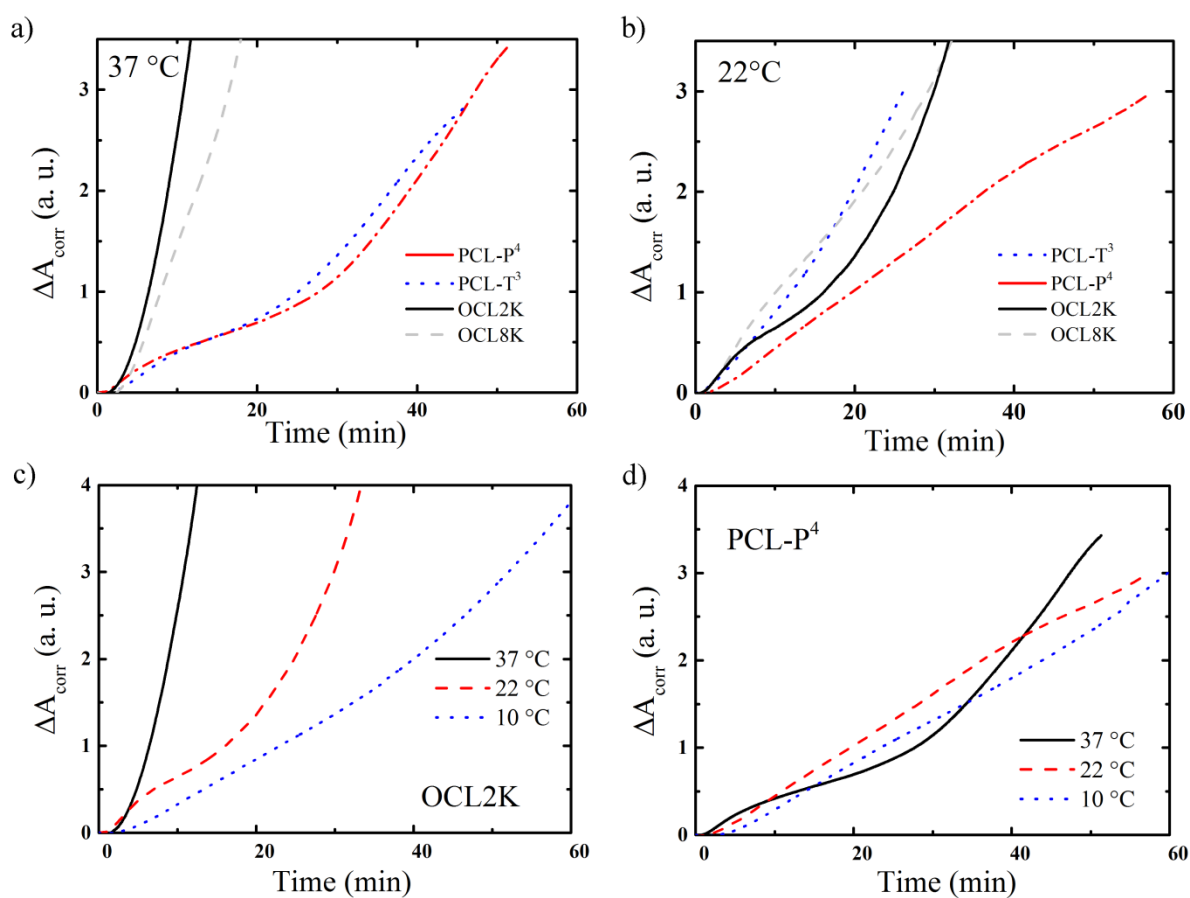

Fig. 4 Corrected surface area (ΔA_{corr}) against the time determined in LMD experiments under isobaric conditions (π = 7 mN·m^{-1}) of a) PCL-T³, PCL-P[4], OCL2K and OCL8K on a PBS

subphase (pH = 7.4) at a) 37 °C, and b) 22 °C with the lipase *Pseudomonas cepacia* and temperature dependent degradation curve for c) OCL2K and d) PCL-P[4].

At 10 °C for the linear OCL2K a slightly slower degradation is observed (Fig. 4c) which agrees with reported data for PCL [30]. This effect was attributed to a reduced activity of the lipase. Surprisingly, for PCL-P[4] (Fig. 4d) only small differences between the different temperatures are found, which could be the result of distinction in the packing motives (larger required space per molecule at 37 °C on buffer solution). The less packed 2D structure leads to an apparent slower degradation despite higher enzyme activities. The different temperature dependences of the enzymatic activities for OCL and PCL-P[4] probably result from the higher amount of ionic (end) groups per repeating OCL segments, because the lipase from *Pseudomonas cepacia* is known for its ability to catalyze hydrophobic systems more than hydrophilic.

From the above presented results, the question arises if the degradation of segmented OCL films at the air-water interface depends in general on the molecular weight of the polymers rather than on the film packing density or on the presence of other parameters. To prove this, we have conducted degradation experiments with P(OCL-U)s containing OCL segments with molecular weight comparable to those of the OCL arms in the star-shape molecules. We have chosen urethane bonds for introducing chain extender units because they are able to modify the packing density in the Langmuir film by forming H-bonds and because the cleavage of the urethane junction units by the lipase from *Pseudomonas cepacia* is not reported. Recently, the surface pressure-induced isothermal transition from 2D to 3D was investigated for different P(OCL-U)s with respect to the influence of urethane junction units on the crystallization and aggregation behavior [33]. The incorporation of urethane linkers derived either from TMDI, HDI or LDI induces changes in the mesoscopic structure of the polymeric Langmuir films and have an impact on the diffusion-limited aggregation kinetics at 22 °C on a pure water

subphase. Below the inflection points no morphologies are detected by BAM either for linear OCL or P(OCL-U). The π-A isotherms of the P(OCL-U)s are recorded at 37 °C on the buffered subphase and reveal the influence of the urethane junction unit on the monolayer behavior compared to non-segmented OCLs (Fig. 5). Increased surface areas at surface pressures lower 8 mN·m^{-1} for all P(OCL-U)s have been found. This observation is in contrast to results obtained at a pure aqueous subphase at 22 °C, where smaller mean molecular area per repeating unit were observed for these copolymers due to enhanced attractive intra- or intermolecular interactions between the urethane/ester function [33]. Since the isotherm for the PCL layer at 22 °C (water) and 37 °C (PBS) is almost the same the shift of the P(OCL-U) isotherms on buffer can only be related to the urethane linker moieties and is attributed to reduced attractive intra- or intermolecular interactions of the macromolecules but more intensive interactions with the cations in the subphase. The enzymatic LMD experiments for OCL and P(OCL-U)s were performed at π = 7 mN·m^{-1} since the values of the inflection points are in the same range for all polymers (Table 3).
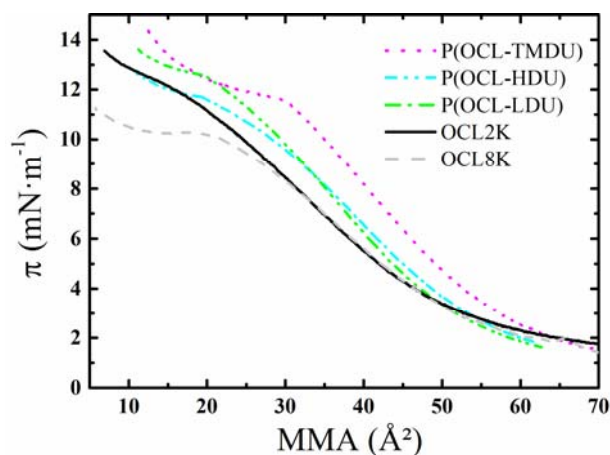

Fig. 5 π-A isotherms at 37 °C on a PBS subphase (pH = 7.4) for P(OCL-TMDU), P(OCL-HDU), P(OCL-LDU), and linear OCL2K and OCL8K.

Table 3 Langmuir monolayer characterization of P(OCL-U) and linear OCL2K by using the MMA$_i$ value [Å^2] and the corresponding surface pressure π_i [mN·m^{-1}] determined at 22 °C on a water subphase and at 37 °C on a PBS buffered subphase.

Sample ID	MMA$_i$	π_i	MMA$_i$	π_i
	water, 22 °C		PBS, 37 °C	
OCL2K	39	6.6	36	6.4
P(OCL-TMDU)	35	6.4	42	7.3
P(OCL-HDU)	31	5.7	39	7.0
P(OCL-LDU)	35	5.5	35	7.6

A significantly slower surface area reduction is observed for all P(OCL-U) layers compared to the OCL films (Fig. 6a-c). Whereas the lower molecular weight OCL Langmuir films degrade under similar experimental conditions very fast ($\Delta A_{corr} \geq 3$ in 30 min), the degradation rates for the P(OCL-U)s are lower than $\Delta A_{corr} \sim 0.2$ in 60 min. For PCL it is known that the ΔA_{corr} values are molecular weight dependent, but PCL Langmuir films with comparable M_n (43,000 g·mol^{-1}) show a significantly faster enzymatic degradation ($\Delta A_{corr} \geq 3$ for 60 min) than the P(OCL-U)s (Fig. 6d) [30].
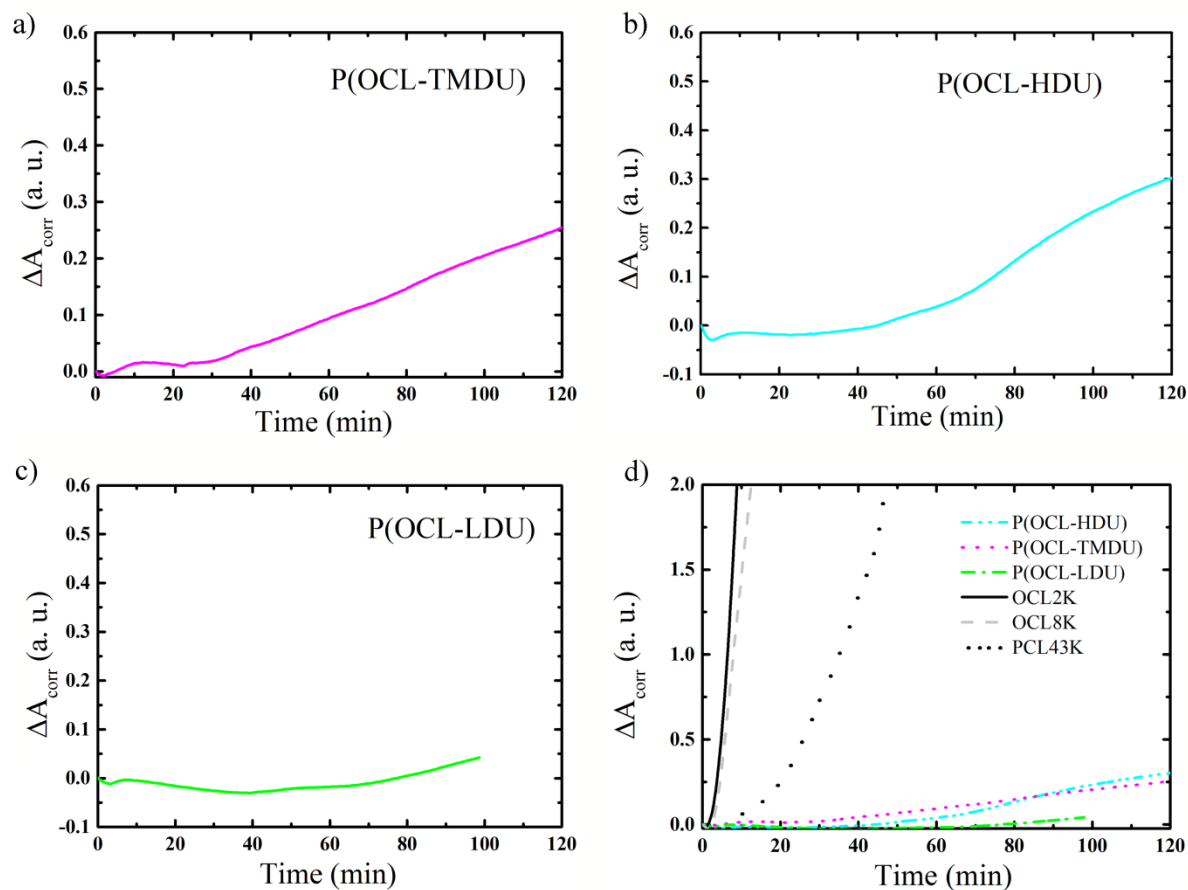
Fig. 6 Corrected surface area (ΔA_{corr}) against the time determined in LMD experiments under isobaric conditions ($\pi = 7$ mN·m^{-1}) of a) P(OCL-TMDU), b) P(OCL-HDU), c) P(OCL-LDU), and d) all P(OCL-U) compared to OCL2K and OCL8K on a PBS subphase (pH = 7.4) at 37 °C sing the lipase from *Pseudomonas cepacia*. Data for the PCL43K curve were extracted from Ref. [30].

By comparing the ΔA_{corr} values for the three different urethane junction units, it becomes apparent that the film with the chain extender LDI, which includes an additional ester side group, exhibits the slowest surface area reduction (Table 4). The obtained values for the P(OCL-LDU) layer are in the same range as for the hydrolytic degradation of PCL ($\Delta A_{corr} \sim$ 0.05 for 60 min) [30].A slower degradation of this particular P(OCL-U) is in good agreement with the knowledge that the lipase from *Pseudomonas cepacia* preferentially cleaves ester bonds in more hydrophobic molecules. It can be concluded from the extremely retarded degradation curves of the P(OCL-U) compared to the high molecular PCL (Fig. 6d) that the retarded degradation of the P(OCL-U) is not caused by the higher molecular weight, but by the varied interactions between the polymers and the enzyme. This explains a direct influence of the urethane junction units on the enzymatic driven process. For PCL based polymers including urea segments it was reported that the enzymatic degradation by the lipase from *Thermomyces lanuginosus* is reduced in bulk experiments [37]. This behavior was ascribed to the introduced hydrogen bonding moieties, which increase the overall polarity, have a stabilizing effect and affect the molecular dynamics. Therefore, we assume that the urethane bonds, which are in direct contact with the subphase, interact with the enzyme dissolved in the subphase changing its orientation or even conformation and the fast random chain scission process as it is known for the degradation of PCL by lipase *Pseudomonas cepacia* is prevented for P(OCL-U).

Table 4 Corrected surface area (ΔA_{corr}) after a degradation time 60 min for P(OCL-TMDU), P(OCL-LDU), and P(OCL-HDU).

Sample ID	ΔA_{corr} 100 min
P(OCL-LDU)	0.05
P(OCL-TMDU)	0.21
P(OCL-HDU)	0.27

All P(OCL-U) films show almost no surface area changes in the first ~40 min after injection of the lipase (Fig. 6). The effect is strongly enhanced at lower temperature, for example for P(OCL-TMDU) the surface area remains almost constant during the degradation time period of 3 h (Fig. 7). This lag time results probably from degradation processes within the films, which do not form water soluble fragments immediately. The incorporation of enzyme molecules within the polymer layer could not be revealed neither by BAM nor by monitoring the film surface area at constant surface pressures.
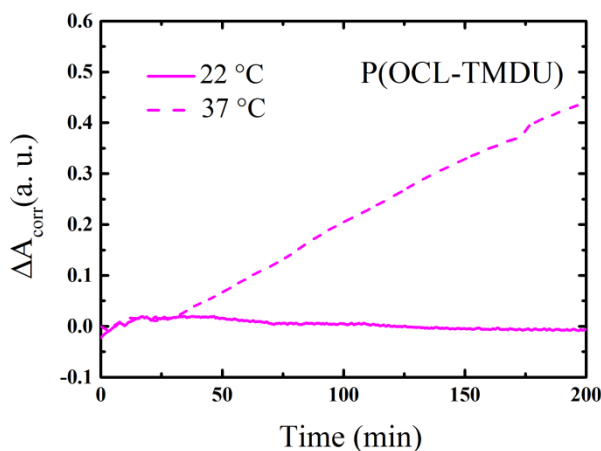

Fig. 7 Corrected surface area (ΔA_{corr}) against the time determined in LMD experiments under isobaric conditions ($\pi = 7$ mN·m^{-1}) of P(OCL-TMDU) on a PBS subphase (pH = 7.4) at 37 °C and 22 °C using the lipase from *Pseudomonas cepacia*.

4 Conclusion

The interfacial properties and the monolayer degradation behavior of star-shaped PCL with three- and four-arms, where the arms have similar molecular weight than the corresponding linear OCL, were investigated. Oligo(ε-caprolactone) based copolyesterurethanes P(OCL-U)s containing OCL segments with molecular weight similar to the arms in the star-shaped

polymers are also included in the study to separate the influence of the molecular weight of OCL segments in the copolymers on the degradation experiments from the influence of the film packing densities. The star-shaped PCL with three- and four-arms form Langmuir monofilms at the air-water interface exhibiting film packing densities different from the linear OCLs. The enhancement of the ionic interactions with the cations in the buffered subphase results in improved inter- and intramolecular repulsions and require higher mean molecular area with increased number of end groups. The molecular architecture also influences the degradability of the Langmuir films during enzymatic LMD experiments with lipase from *Pseudomonas cepacia* at relevant biological conditions of 37 °C on a PBS buffer subphase. The degradation rate for both three- and four-arm PCL is significantly reduced compared to the linear OCL although the film packing densities are lower. The retarded film degradation is not related to the molecular weights of the star-shaped polymers but to their enhanced hydrophilic character resulting from the formation of partially charged stars. Interestingly, our LMD results at 22 °C confirm bulk degradation experiments of star-shaped PCL at 37 °C in buffer showing the LMD as simple and fast but powerful method to gain knowledge about the enzymatic polymer degradation.

P(OCL-U) consisting of OCL segments with similar molecular weight as the linear OCL and star-shaped PCLs linked with urethane junctions units as chain extender exhibit a significant retarded degradation behavior in comparison to linear OCL. The lower enzymatic degradation rate of P(OCL-U) films at the air-water interface is clearly related to the modified inter- and intramolecular interactions between the copolymer monofilm and the enzyme molecules and not to the molecular weight of the copolymers and the film packing density.

In summary, independent of the molecular weight of the polymer and oligomers and their packing densities the enzymatic degradation of the Langmuir film by the lipase from *Pseudomonas cepacia* is adjusted by even slightly modified hydrophilicity of the molecules. Whereas for star-shaped PCL the polarity of the end group is responsible for the reduced

degradation rate, in P(OCL-U) the hydrophilic ester side groups have this effect. Moreover, in P(OCL-U) the stronger interaction with the urethane bonds properly prevent the catalytic reaction of the enzyme.

Our results reveal that the LMD technique allows the parallel analyses of both the film enzyme interactions and the degradation process on the molecular level.

Acknowledgement

Appendix A. Supplementary data

Supplementary data related to this article can be found at http://dx.doi.org/10.1016/j.polymdegradstab.2016.07.010.

References

1. L. S. Nair and C. T. Laurencin, *Progress in Polymer Science*, 2007, **32**, 762-798.
2. J. Choi, I.-K. Kim and S.-Y. Kwak, *Polymer*, 2005, **46**, 9725-9735.
3. H. Y. Li, R. Riva, H. R. Kricheldorf, R. Jerome and P. Lecomte, *Chem-Eur J*, 2008, **14**, 358-368.
4. D. J. A. Cameron and M. P. Shaver, *Chem Soc Rev*, 2011, **40**, 1761-1776.
5. L. Qiu and Y. Bae, *Pharm Res*, 2006, **23**, 1-30.
6. R. Kodiyath, I. Choi, B. Patterson, C. Tsitsilianis and V. V. Tsukruk, *Polymer*, 2013, **54**, 1150-1159.
7. J.-L. Wang and C.-M. Dong, *Polymer*, 2006, **47**, 3218-3228.
8. W. Xie, N. Jiang and Z. Gan, *Macromolecular Bioscience*, 2008, **8**, 775-784.
9. J.-L. Wang, L. Wang and C.-M. Dong, *J Polym Sci A: Polym Chem*, 2005, **43**, 5449-5457.
10. A. L. Sisson, D. Ekinci and A. Lendlein, *Polymer*, 2013, **54**, 4333-4350.
11. M. Behl, U. Ridder, Y. Feng, S. Kelch and A. Lendlein, *Soft Matter*, 2009, **5**, 676-684.
12. K. Chavalitpanya and S. Phattanarudee, *Energy Procedia*, 2013, **34**, 542-548.
13. J. Kloss, M. Munaro, G. P. De Souza, J. V. Gulmine, S. H. Wang, S. Zawadzki and L. Akcelrud, *J Polym Sci A: Polym Chem*, 2002, **40**, 4117-4130.
14. B. Bogdanov, V. Toncheva, E. Schacht, L. Finelli, B. Sarti and M. Scandola, *Polymer*, 1999, **40**, 3171-3182.
15. B. Bogdanov, V. Toncheva and E. Schacht, *J Therm Anal Calorim*, 1999, **56**, 1115-1121.
16. Z. Gan, Q. Liang, J. Zhang and X. Jing, *Polym Degrad Stabil*, 1997, **56**, 209-213.
17. N. Grozev, A. Svendsen, R. Verger and I. Panaiotov, *Colloid Polym Sci*, 2002, **280**, 7-17.
18. L. Q. Yang, J. X. Li, Y. Jin, M. Li and Z. W. Gu, *Polym Degrad Stabil*, 2015, **112**, 10-19.
19. K. E. Jaeger, A. Steinbuchel and D. Jendrossek, *Appl Environ Microb*, 1995, **61**, 3113-3118.
20. Z.-M. Miao, S.-X. Cheng, X.-Z. Zhang, Q.-R. Wang and R.-X. Zhuo, *J Biomed Mater Res B: Appl Biomater*, 2007, **81B**, 40-49.
21. K. Lemke, M. Lemke and F. Theil, *J Org Chem*, 1997, **62**, 6268-6273.
22. J. D. Schrag, Y. G. Li, M. Cygler, D. M. Lang, T. Burgdorf, H. J. Hecht, R. Schmid, D. Schomburg, T. J. Rydel, J. D. Oliver, L. C. Strickland, C. M. Dunaway, S. B. Larson, J. Day and A. McPherson, *Structure*, 1997, **5**, 187-202.
23. D. A. Lang, M. L. M. Mannesse, G. H. De Haas, H. M. Verheij and B. W. Dijkstra, *Europ J Biochem*, 1998, **254**, 333-340.
24. I. Luzinov, S. Minko and V. V. Tsukruk, *Prog Polym Sci*, 2004, **29**, 635-698.
25. I. W. Hamley, *Prog Polym Sci*, 2009, **34**, 1161-1210.
26. L. Zhao and Z. Q. Lin, *Soft Matter*, 2011, **7**, 10520-10535.
27. J. Reiche, K. Kratz, D. Hofmann and A. Lendlein, *Int J Artif Organs*, 2011, **34**, 123-128.
28. J. K. Lee, J. H. Ryon, W. K. Lee, C. Y. Park, S. B. Park and S. K. Min, *Macromol. Res.*, 2003, **11**, 476-480.
29. A. Kulkarni, J. Reiche and A. Lendlein, *Surf Interface Anal*, 2007, **39**, 740-746.
30. A. Kulkarni, J. Reiche, K. Kratz, H. Kamusewitz, I. M. Sokolov and A. Lendlein, *Langmuir*, 2007, **23**, 12202-12207.
31. A. Leiva, L. Gargallo and D. Radić, *J Macromol Sci, Part A*, 2004, **41**, 577-583.

32.   T. J. Joncheray, K. M. Denoncourt, C. Mathieu, M. A. R. Meier, U. S. Schubert and R. S. Duran, *Langmuir*, 2006, **22**, 9264-9271.
33.   A.-C. Schöne, K. Kratz, B. Schulz, J. Reiche, S. Santer and A. Lendlein, *Polym Advan Technol*, 2015, **26**, 1411-1420.
34.   J. Zotzmann, M. Behl, D. Hofmann and A. Lendlein, *Adv Mater*, 2010, **22**, 3424-3429.
35.   Y. Chatani, Y. Okita, H. Tadokoro and Yamashit.Y, *Polym J*, 1970, **1**, 555-&.
36.   H. L. Hu and D. L. Dorset, *Macromolecules*, 1990, **23**, 4604-4607.
37.   M. C. P. Brugmans, S. H. M. Söntjens, M. A. J. Cox, A. Nandakumar, A. W. Bosman, T. Mes, H. M. Janssen, C. V. C. Bouten, F. P. T. Baaijens and A. Driessen-Mol, *Acta Biomater*, 2015, **27**, 21-31.